Accuracy and Precision of a New H/D Exchange- and Mass Spectrometry-Based Technique for Measuring the Thermodynamic Properties of Protein−Peptide Complexes

Kendall D. Powell and Michael C. Fitzgerald*

Department of Chemistry, Duke University, Durham, North Carolina 27708

Received January 17, 2003; Revised Manuscript Received February 17, 2003

ABSTRACT: A new H/D exchange- and MALDI mass spectrometry-based technique, termed SUPREX, was used to characterize the thermodynamic properties of a series of model protein−peptide complexes of the Abelson tyrosine kinase SH3 domain (abl-SH3) and the S-Protein (S-Pro). The SUPREX technique was employed to evaluate the folding free energies (ΔG_f values) of each model protein in the absence and in the presence of a series of different peptide ligands. Ultimately, these SUPREX-derived ΔG_f values were used to calculate dissociation constants (K_d values) for each of the nine protein−peptide complexes in this study. As part of this work, we describe a new data collection and analysis method that allows the accurate and precise determination of protein folding *m*-values in the SUPREX experiment. The *m*-values that we determined for the abl-SH3 domain and the S-Pro system were in good agreement with those determined by conventional techniques. Our results also indicate that the SUPREX-derived K_d values for the protein−peptide complexes in this work were in reasonably good agreement with those determined by conventional techniques.

Many different areas of biochemical research require the accurate measurement of protein−peptide binding constants. Such measurements are important for understanding the many cellular processes that involve protein−peptide complexes (*1*−*5*). They are also often used to understand the detailed molecular interactions that mediate protein−protein interactions in the cell (*6*−*9*). Conventional techniques for characterizing the thermodynamic properties of protein−peptide complexes typically rely on the use of various optical spectroscopies or the use of calorimetric methods. These approaches have been widely used over the years to study the thermodynamic properties of many different types of protein−peptide interactions; however, they lack several capabilities. For example, they are not amenable to the analysis of small amounts of protein, to the study of proteins in complex biological mixtures, or to characterization of protein−peptide complexes in a high throughput fashion.

Recently, we introduced a mass spectrometry- and H/D exchange-based technique that can be used to determine the thermodynamic stability (i.e., ΔG_f) of a protein (*10*). This technique, which we have termed SUPREX (stability of unpurified proteins from rates of H/D exchange), can be used to determine the ΔG_f values of a wide variety of proteins both in vitro and in vivo with high precision and good accuracy (*10*−*14*). Significantly, the SUPREX technique requires only a small amount of material, and it is amenable to the analysis of proteins in complex mixtures. Recently, we have also demonstrated that the SUPREX technique can be used to measure the increase in a protein's ΔG_f value upon ligand binding and that this increase in a protein's ΔG_f value upon ligand binding can be used to evaluate protein−ligand binding constants (*15*).

Our recent report on the use of SUPREX for measuring protein−ligand binding constants included the analysis of one protein−peptide complex (i.e., the noncovalent complex formed between the S-Protein (S-Pro)[1] and the S-Peptide (S-Pep)). In that report, the SUPREX-derived K_d value we obtained for the S-Pro/S-Pep complex, 2.4 nM, was in reasonably good agreement with the K_d value of 1.1 nM previously established by conventional methods. Here, we report the SUPREX-derived K_d values of eight additional protein−peptide complexes for which K_d values have been previously determined by conventional methods. The model protein−peptide complexes in this study include a series of protein−peptide complexes involving the 61-amino acid SH3 domain from the Abelson tyrosine kinase (abl-SH3) and a series of protein−peptide complexes involving the 104-amino acid S-Pro. The abl-SH3 domain is known to bind a variety of proline-containing peptides (*6*, *7*), and S-Pro is known to bind a variety of different α-helical peptides (*16*−*21*).

The goal of this study was to assess the accuracy and precision of the SUPREX technique for measuring the strength of protein−peptide interactions. As part of this work,

* Corresponding Author: Dr. Michael C. Fitzgerald, Department of Chemistry, Box 90346, Duke University, Durham, NC 27708-0346. Tel: 919-660-1547. Fax: 919-660-1605. E-mail: michael.c.fitzgerald@duke.edu.

[1] Abbreviations: S-Pro = the S-Protein component of RNase S (residues 21−124 of bovine pancreatic ribonuclease A); S-Pep = the S-Peptide component of RNase S (residues 1−20 of bovine pancreatic ribonuclease A); abl-SH3 = the Src homology domain 3 from the Abelson tyrosine kinase; ΔG_f = protein folding free energy in the absence of denaturant; [Denaturant] = molar denaturant concentration; $C_{SUPREX}^{1/2}$ = [Denaturant] at the midpoint of a SUPREX curve; MALDI-TOF = matrix assisted laser desorption/ionization-time-of-flight mass spectrometer.

10.1021/bi034096w CCC: $25.00
Published on Web 04/08/2003

we describe a new strategy for the acquisition and analysis of SUPREX data. This new strategy provides a useful means by which to experimentally determine the "*m*-value" (i.e., $\delta\Delta G_f/\delta$[Denaturant]) of a protein folding reaction with good accuracy and precision. The accurate determination of such *m*-values is important for understanding the thermodynamic properties of proteins and protein−peptide complexes.

EXPERIMENTAL SECTION

Reagents. Deuterium oxide (D_2O; 99.9% atom D), deuterium chloride (20 wt % in D_2O, 99.5% atom D), and sodium deuteroxide (40 wt % in D_2O, 99.9% atom D) were purchased from Aldrich. Urea was purchased either from Mallinckrodt (ACS grade) or ICN Biomedicals (Ultrapure). Deuterated urea (urea-d_4) was prepared by repeated dissolution and lyophilization of fully protonated urea in D_2O until the calculated deuterium content was >99%. Sinapinic acid (SA) was obtained from either Aldrich or Sigma. Trifluoroacetic acid (TFA) was from Halocarbon, and acetonitrile (MeCN) and methanol (MeOH) were from Fisher. Bovine pancreatic ribonuclease A (RNase A), subtilisin Carlsberg, and hen egg white lysozyme were all from Sigma.

General Methods and Instrumentation. MALDI mass spectra were acquired on either a Voyager DE (Perseptive Biosystems) or a Voyager DE-Pro Biospectrometry Workstation (Applied Biosystems). Spectra were collected on both instruments in the linear mode using a nitrogen laser (337 nm). SUPREX samples were prepared for MALDI analysis as described below. SA was the matrix in all experiments. Positive ion mass spectra were collected either manually or in the autosampler mode using the following parameters: 25 kV acceleration voltage, 23.25 or 23.5 kV grid voltage for S-Pro and SH3 analyses, respectively, 75 V guide wire voltage, and 225 ns delay time. Each mass spectrum obtained was the sum of about 20−25 laser shots. Raw MALDI spectra were processed with an in-house Microsoft Excel macro that performed the following operations: a 19-point floating average smoothing of the data, a two-point mass calibration of the spectra using the protein ion signals from the internal mass calibrants, and a center of mass determination for the protein's $[M+H]^{+1}$ peak.

A Hewlett-Packard 8452A Diode Array UV/Vis spectrophotometer was used for protein concentration determinations. Abl-SH3 concentrations were determined using absorbance measurements at 280 nm ($\varepsilon_{280} = 15470\ M^{-1}\ cm^{-1}$ (W. Lu, personal communication)). S-Pro concentrations were determined using absorbance measurements at 280 nm ($\varepsilon_{280} = 9800\ M^{-1}\ cm^{-1}$) (*16*). The exact peptide ligand concentrations in this work were established by quantitative amino acid analysis (AAA Laboratories; Mercer Island, WA) after acid hydrolysis. Urea concentrations were determined with a Bausch & Lomb refractometer as described (*22*). pH measurements were performed with a Jenco 6072 pH meter equipped with a Futura calomel pH electrode from Beckman Instruments. To correct for isotope effects, the measured pH of each D_2O solution was converted to pD by adding 0.4 to the measured pH value (*23*).

Protein and Peptide Samples. The abl-SH3 domain was prepared by total chemical synthesis and kindly provided in purified form from by Professor Wuyuan Lu at the University of Maryland. The abl-SH3 domain was folded by dissolving ~0.5 mg of the pure lyophilized material in 200 μL of water. After the sample was vigorously vortexed, the solution was centrifuged at 10000*g* for 5 min to remove the insoluble portion of the sample. Ultimately, the supernatant was removed and stored at 4 °C until needed.

Table 1: Amino Acid Sequences of the Abl-SH3 Domain and S-Pro Peptide Ligands Used in These Studies

Peptide Number	Peptide Sequence[a]
abl-SH3 Ligands	
1	APT**R**SPPPPP
2	APT**F**SPPPPP
3	APTYSPPPPP
4	APT**W**SPPPPP
S-Pro Ligands	
5	**ac-**Y**E**TAAAKFER**P**H**V**DS**-NH$_2$**
6	K**E**TAAAKFERQH**A**DS**-NH$_2$**
7	**ac-**Y**E**TAA**P**KFERQH**V**DS**-NH$_2$**
8	K**E**TAAAKFERQH**X**DS**-NH$_2$**
9	KETAAAKFERQHMDSSTSAA

[a] Peptide 3 is identical to peptide P40 from ref *6*; this is taken to be the "wild-type" ligand for the abl-SH3 domain. Peptide 9 is the wild-type, 20 amino acid S-Pep. Mutations with respect to the wild-type peptide sequences are shown in boldface. Abbreviations are ac- = acetylation, -NH_2 = amidation, and X = the unnatural amino acid, norleucine. Peptides 5 and 7 were very similar to the Q11P and A6P peptides, respectively, from ref *21*. Peptides 6 and 8 were identical to the M13A and M13Nle peptides from refs *17* and *18*, respectively.

RNase S was prepared from RNase A by using subtilisin Carlsberg to selectively cleave the peptide bond between residues 20 and 21 of RNase A as previously described (*24*). The two major peptide fragments formed in the proteolysis reaction were the S-Pep fragment which included residues 1−20 of RNase A (see peptide 9 in Table 1) and the S-Pro fragment which included residues 21−124 of RNase A. Ultimately, these two fragments were purified from the digest and from each other by semipreparative RP-HPLC using a 10−50% linear gradient of buffer A in B (buffer A = 90% MeCN in water containing 0.09% TFA and buffer B = 0.1% TFA in water) over 30 min. The RP-HPLC fractions that contained pure S-Pro as judged by ESI mass spectrometry were combined and lyophilized as were the RP-HPLC fractions that contained pure peptide 9. S-Pro was folded by dissolution of the pure, lyophilized product in a 50 mM sodium acetate buffer (pH 6.0) containing 100 mM NaCl.

Table 1 shows the names and amino acid sequences of the peptides used in this study. Peptides 1−4 were synthesized, purified, and kindly provided as lyophilized solids by Professor Wuyuan Lu. Peptide 9 corresponds to the wild-type sequence of the S-Pep fragment and was prepared by the proteolysis procedure described above. Peptides 5−8 were synthesized in our laboratory using standard methods for manual solid-phase peptide synthesis (SPPS) and in situ neutralization protocols for *tert*-butoxycarbonyl (Boc) chemistry as described elsewhere (*25*). We note that all the synthetic peptides in this work were prepared with C-terminal carboxyl groups and N-terminal amino groups with the exceptions that peptides 5−8 were prepared with C-terminal amide groups and that peptides 5 and 7 were acetylated at their N-termini. Each synthetic peptide in this study (including those obtained from Professor Lu) was purified by semipreparative RP-HPLC. The mass of each peptide as determined by ESI mass spectrometry was within 0.2 Da of the theoretical mass.

SUPREX Sample Preparation and Data Collection. Concentrated stock solutions of S-Pro and of peptides 5−9 were

prepared in 50 mM sodium acetate buffers (pH 6.0) containing 100 mM NaCl. Protein−peptide complexes involving S-Pro and peptides 5−9 were prepared by combining aliquots of the S-Pro stock solution with each peptide stock solution to yield solutions of each S-Pro/peptide complex in which the final S-Pro concentration was 100 μM and the final peptide concentration was between 0.8 and 2.0 mM. The exact concentration of peptide in each solution was determined as described above. Each S-Pro/peptide stock solution was allowed to equilibrate for at least 1 h at room temperature before it was cooled to 10 °C.

SUPREX analyses on the S-Pro and S-Pro/peptide complexes in this work were initiated by 10-fold dilution of the above stock solutions of protein or protein−peptide samples into a series of deuterated exchange buffers. The deuterated exchange buffers contained 50 mM sodium acetate buffer (pD 6.0), 100 mM NaCl, and concentrations of urea-d_4 that varied between 0 and 7 M. After a specific exchange time (see below), a 1 μL aliquot of each protein-containing exchange buffer was combined with 9 μL of an ice-cold, MALDI matrix solution which also included an internal mass standard. The matrix solution consisted of a saturated, aqueous solution of SA containing 45% MeCN and 0.1% TFA (pH ~3.0). The low temperature and low pH of the matrix solution effectively quenched the H/D exchange reaction. Subsequently, 1 μL of the quenched exchange solution was spotted on a stainless steel MALDI plate and the solvent was evaporated under a gentle flow of air. A total of 10 replicate spectra were collected from various regions of the crystalline MALDI sample spot to determine the average mass change (relative to a fully protonated sample) at each concentration of urea. Ultimately, the mass change relative to a fully protonated sample (i.e., ΔMass) was plotted as a function of [Denaturant].

Concentrated stock solutions of the abl-SH3 domain and of peptides 1−4 were prepared in 10 mM sodium phosphate buffers (pH 7.4) containing 10 mM dithiothreitol. Protein−peptide complexes involving the abl-SH3 domain and peptides 1−4 were prepared by combining aliquots of the abl-SH3 domain stock solution with each peptide stock solution to yield solutions of each abl-SH3/peptide complex in which the final abl-SH3 concentration was 20 μM and the final peptide concentration was about 2.0 mM. The exact concentration of peptide in each solution was determined as described above. Each abl-SH3/peptide stock solution was allowed to equilibrate for at least 1 h before it was cooled to 20 °C.

SUPREX analyses on the abl-SH3 domain and abl-SH3 domain/peptide complexes in this work were performed using a protocol that was essentially identical to that described above for the S-Pro system with the exceptions that 10 μL, C_4 ZipTip pipet tips (Millipore) were employed for optimum sample economy and that a 12-channel pipettor was used to reduce the amount of time required for the pipetting steps in our analyses. The C_4 ZipTip pipet tips in this work were specifically used to concentrate and desalt the protein samples in the deuterated exchange buffers. This was accomplished exactly as described in ref *12*. We note that the series of deuterated exchange buffers used in the abl-SH3 domain experiments contained 10 mM sodium phosphate (pD 7.4) and concentrations of urea-d_4 that varied between 0 and 5 M.

SUPREX Data Analysis. Plots of ΔMass versus [urea] were constructed for the S-Pro and abl-SH3 domain in the absence and in the presence of their respective ligands, and the data were fit to the following four-parameter sigmoidal equation using a nonlinear regression routine in Sigma Plot.

$$\Delta\text{Mass} = \Delta M_o + \frac{a}{1 + e^{-(([\text{Denaturant}] - C_{1/2}^{\text{SUPREX}})/b)}} \quad (1)$$

In eq 1, ΔM_o is the change in mass measured before the globally protected hydrogens in the protein exchanged with deuterons (i.e., the pretransition baseline); a is the amplitude of the curve in Da; [Denaturant] is the molar denaturant concentration; $C_{\text{SUPREX}}^{1/2}$ is the [Denaturant] at the transition midpoint of the curve; and b is a parameter that describes the steepness of the transition. In fitting our ΔMass vs [Denaturant] data sets to eq 1 all of the parameters in the equation were typically allowed to "float."

The $C_{\text{SUPREX}}^{1/2}$ values we obtained using eq 1 were then used in eq 2 to determine m and ΔG_f values. In eq 2, R is

$$-RT\left[\ln\frac{\left(\frac{\langle k_{\text{int}}\rangle t}{0.693} - 1\right)}{\left(\frac{n^n}{2^{n-1}}[\text{P}]^{n-1}\right)}\right] = mC_{\text{SUPREX}}^{1/2} + \Delta G_f \quad (2)$$

the gas constant, T is the temperature in Kelvin, $\langle k_{\text{int}}\rangle$ is the average intrinsic exchange rate of an amide proton, t is the H/D exchange time, n is the number of subunits in the protein (for the proteins in this work $n = 1$), [P] is the protein concentration expressed in n-mer equivalents, m is defined as $\delta\Delta G_f/\delta$[Denaturant], and ΔG_f is the free energy of folding in the absence of denaturant. We note that eq 2 is valid only for cases in which the product $\langle k_{\text{int}}\rangle t$ is greater than 0.693 and for finite values of t such that $C_{\text{SUPREX}}^{1/2}$ values are greater than or equal to 0 M denaturant. Equation 2 also requires that the protein under study be under so-called EX2 exchange conditions and that the chemical denaturant-induced equilibrium unfolding properties of the protein be well modeled by a two-state process. A derivation of eq 2 is included in the appendix.

We have previously reported on the use of eq 2 to calculate a protein's ΔG_f value from SUPREX data (*13*). However, in these earlier studies the only experimentally determined parameter in eq 2 was $C_{\text{SUPREX}}^{1/2}$. All the other parameters were either predefined (as in the case of R, T, and t) or estimated (as in the case of $\langle k_{\text{int}}\rangle$ and m). Of particular note in our earlier work was that the m-values employed in our calculations of ΔG_f values using eq 2 were estimated using an empirically derived relationship between the number of amino acid residues in a protein and the magnitude of a protein's m-value (*26*).

In the work described here, all m-values were experimentally determined from SUPREX data. This was accomplished by generating a series of SUPREX curves using different H/D exchange times (i.e., t values in eq 2). SUPREX curves for the abl-SH3 domain protein−peptide systems and the S-Pro protein−peptide systems were collected using exchange times between 5 and 72 min and between 10 and 4575 min, respectively. Increasing the H/D exchange time in a SUPREX experiment has the effect of shifting the

observed $C_{SUPREX}^{1/2}$ value of a protein's SUPREX curve to lower concentrations of denaturant. Our experimental determination of *m*-values in this work involved generating a plot in which the term on the left side of eq 2 was plotted as a function of the observed $C_{SUPREX}^{1/2}$ value. In evaluating the term on the left side of eq 2, values for $\langle k_{int} \rangle$ were obtained by using the program SPHERE (*27*, *28*). The SPHERE program calculates the intrinsic H/D exchange rate (i.e., k_{int}) of each individual backbone amide proton in a protein based on exchange data from model dipeptide studies (see ref 28). These k_{int} values are averaged to obtain the $\langle k_{int} \rangle$ value in eq 2. Ultimately, a linear least-squares analysis of the data in these plots yielded the equation of a line in which the slope and *y*-intercept corresponded to *m* and ΔG_f, respectively.

K_d Value Determinations. Dissociation constants, K_d values, for the protein−peptide complexes studied in this work were calculated using eq 3 (*29*).

$$K_d = [L]/(e^{-\Delta\Delta G_f/nRT} - 1) \quad (3)$$

In eq 3, [L] is the concentration of free peptide, *n* is the number of independent binding sites, and $\Delta\Delta G_f$ is the change in folding free energy upon peptide binding. For the model protein systems in this study, it has been previously established that there is a single peptide binding site ($n = 1$). In our binding experiments with the abl-SH3 domain, there was a large excess of ligand, therefore [L] was taken as the total concentration of peptide in solution. In our binding experiments with S-Pro, the peptide ligands were present in less than a 10-fold excess over the protein concentration; therefore eq 4 was used together with eq 3 to calculate K_d values (*30*). In eq 4, L_{total} is the total concentration of peptide; P_{total} is the total concentration of S-Pro; and K_d is the dissociation constant for the complex.

$$[L] = L_{total} - \frac{P_{total} + L_{total} + K_d - \sqrt{(P_{total} + L_{total} + K_d)^2 - 4P_{total}L_{total}}}{2} \quad (4)$$

Conventional Equilibrium Unfolding Study of S-Protein. A 10 μM stock solution of folded S-Pro in 50 mM sodium acetate buffer (pH 6.0) containing 100 mM NaCl was combined with a 10 μM stock solution of unfolded S-Pro in a 50 mM sodium acetate buffer (pH 6.0) containing 100 mM NaCl and 8.9 M urea to create a series of S-Pro solutions that varied only in urea concentration. These solutions were allowed to equilibrate at room temperature for at least 2 h before they were cooled to 10 °C in a water bath. The fluorescence intensity of each solution was recorded 10 times using a Fluorolog-3 fluorimeter (Jobin Yvon-SPEX). In these experiments, the excitation wavelength was 278 nm, the emission wavelength was 308 nm, the excitation slit width was 10 nm, the emission slit width was 5 nm, and the integration time was 0.2 s. The cuvette was maintained at 10 °C during fluorescence measurements.

The average fluorescence intensity of each solution was plotted as a function of [urea]; and the data were normalized to an apparent fraction of unfolded protein (F_{app}) according to eq 5 (*22*):

$$F_{app} = (S - S_F)/(S_F - S_U) \quad (5)$$

where *S* was the fluorescence signal when the protein was equilibrated at a given urea concentration, and S_F and S_U were the respective signals of the folded and unfolded forms of the protein at each urea concentration. In our experiments, *S* was linearly dependent on the urea concentration in both the folded and unfolded baseline regions; therefore, linear extrapolations from these baselines were used to calculate S_F and S_U values. Ultimately, F_{app} values in the transition region of the unfolding curve were converted to ΔG_{app} values using eq 6 (*22*):

$$\Delta G_{app} = -RT \ln[F_{app}/(1 - F_{app})] \quad (6)$$

where ΔG_{app} is the apparent free energy of unfolding at a each urea concentration. The ΔG_{app} values were then used to generate a ΔG_{app} vs. [urea] plot. The data in this plot were fit to eq 7 using a linear least-squares analysis to yield an *m*-value and ΔG_f (*22*).

$$\Delta G_{app} = m[\text{Denaturant}] - \Delta G_f \quad (7)$$

RESULTS

The abl-SH3 domain and the S-protein were subjected to multiple SUPREX analyses in the absence and in the presence of a series of different peptide ligands (see Table 1). In these multiple SUPREX analyses of each protein and protein−peptide complex, the H/D exchange time was varied. Shown in Figures 1 and 2 are typical SUPREX curves obtained for the abl-SH3 domain and for S-Pro with and without a peptide ligand. The solid lines in Figures 1 and 2 represent the best fit of the data to eq 1 using a nonlinear least-squares analysis. We note that the error associated with our ΔMass measurements was typically 2−3 Da, consistent with the mass accuracy of MALDI-TOF mass spectrometry. The fits were used to extract a $C_{SUPREX}^{1/2}$ value for each curve. As predicted by eq 2, the $C_{SUPREX}^{1/2}$ values observed for each protein and protein−peptide complex were shifted to lower denaturant concentrations when longer H/D exchange times were used in the SUPREX experiment.

The pretransition baselines of the SUPREX curves in Figures 1 and 2 were shifted to higher ΔMass values when longer H/D exchange times were employed in the SUPREX experiment. These shifts in the pretransition baselines of our S-Pro and SH3 domain SUPREX curves are likely due to H/D exchange reactions that occur as a result of local unfolding events in these proteins. However, it is important to note that such H/D exchange reactions are not expected to impact our SUPREX analyses. The H/D exhange rates that are measured in our SUPREX experiment are the H/D exchange rates of amide protons which exchange when the protein globally unfolds. It is the H/D exchange rates of these globally protected amide protons that are highly denaturant dependent and ultimately define the transition region of our SUPREX curves.

For each protein and protein−peptide complex we generated a plot of $-RT \ln(\langle k_{int} \rangle t/0.693 - 1)$ versus the observed $C_{SUPREX}^{1/2}$ values. The plots we generated for the abl-SH3 domain and for S-Pro are shown in Figures 3 and 4, respectively. Also shown in Figures 3 and 4 are the plots we obtained when the abl-SH3 domain was bound to peptide

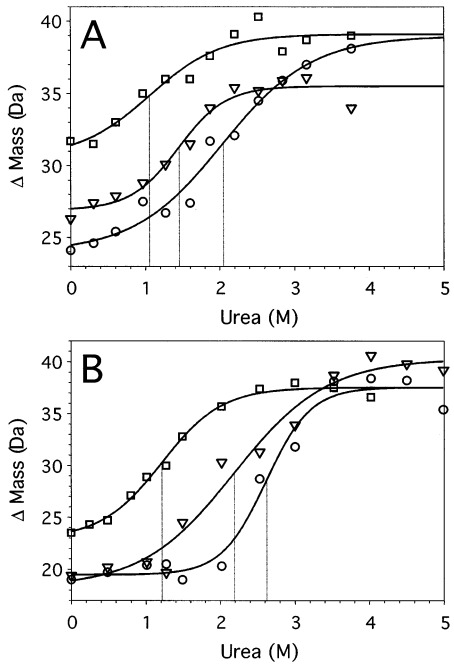

FIGURE 1: (A) Representative SUPREX curves for the abl-SH3 domain (2 μM) in the absence of peptide ligand. H/D exchange times of 5 (circles), 7.5 (triangles), and 13.5 min (squares) resulted in $C_{SUPREX}^{1/2}$ values of 2.04, 1.44, and 1.06 M urea, respectively. (B) Representative SUPREX curves for the abl-SH3 domain (2 μM) in the presence of peptide 3 (180 μM). H/D exchange times of 10 (circles), 20 (triangles), and 65 min (squares) resulted in $C_{SUPREX}^{1/2}$ values of 2.62, 2.19, and 1.21 M urea, respectively. The solid lines represent the best fit of each SUPREX curve to eq 1. The dotted lines mark the $C_{SUPREX}^{1/2}$ values.

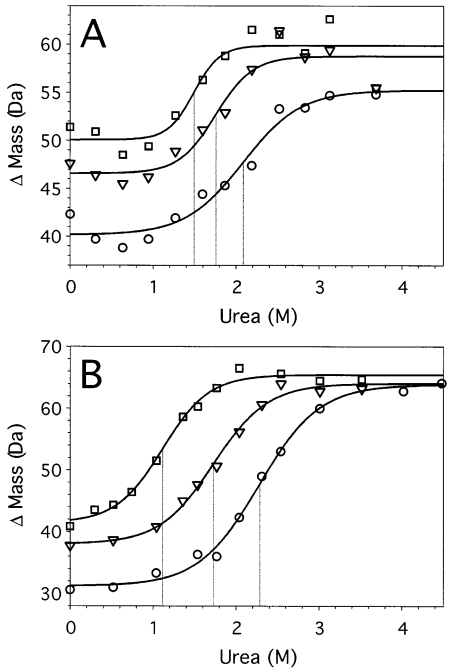

FIGURE 2: (A) Representative SUPREX curves for S-Pro (10 μM) in the absence of peptide ligand. H/D exchange times of 10 (circles), 20 (triangles), and 30 min (squares) resulted in $C_{SUPREX}^{1/2}$ values of 2.08, 1.76, and 1.49 M urea, respectively. (B) Representative SUPREX curves for S-Pro (10 μM) in the presence of peptide 7 (67 μM). H/D exchange times of 25 (circles), 85 (triangles), and 312 min (squares) resulted in $C_{SUPREX}^{1/2}$ values of 2.28, 1.73, and 1.12 M urea, respectively. The solid lines represent the best fit of each SUPREX curve to eq 1. The dotted lines mark the $C_{SUPREX}^{1/2}$ values.

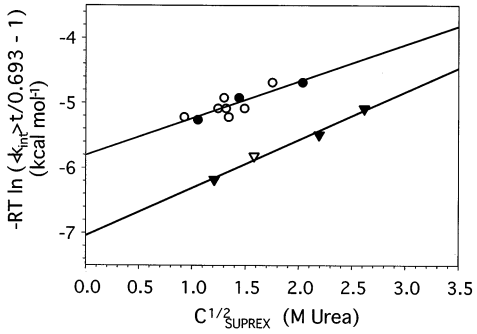

FIGURE 3: The $-RT\ \ln(\langle k_{int}\rangle t/0.693 - 1)$ versus $C_{SUPREX}^{1/2}$ plot obtained for the abl-SH3 domain in the absence (circles) and in the presence (triangles) of peptide 3. Filled symbols indicate the data points from the SUPREX curves shown in Figure 1. The open symbols indicate the data points from additional SUPREX curves (data not shown). The solid lines are the results of linear least-squares fitting of the data to eq 2.

3 (Figure 3) and the S-Pro was bound to peptide 7 (Figure 4). The lines in each plot represent the best fit of the data to a straight line. According to eq 2, the slope and *y*-intercept of each line correspond to the *m*-value and ΔG_f (respectively) of each protein and protein−peptide complex. The *m* and ΔG_f values we obtained from the data in Figures 3 and 4 are summarized in Table 2. Also included in Table 2 are the *m* and ΔG_f values that we obtained in similar analyses on the abl-SH3 domain and S-Pro when they were complexed with several additional peptide ligands (data not shown). The ΔG_f values we calculated in Table 2 were used to calculate $\Delta\Delta G_f$ values for each protein−peptide complex. Ultimately, these $\Delta\Delta G_f$ values were used in eq 3 to determine a SUPREX-derived K_d value for each protein−peptide complex.

The calculation of ΔG_f values from SUPREX data using eq 2 requires that the protein under study exhibit so-called EX2 (and not EX1) exchange behavior. In the EX2 exchange limit, only one population of deuterated protein molecules is typically detected by mass spectrometry during the time course of H/D exchange. This is in contrast to what is observed under so-called EX1 exchange conditions when a protein's refolding rate (k_f) is much slower than $\langle k_{int}\rangle$. In the EX1 exchange limit, two distinct populations of deuterated protein molecules, one in which all of the globally protected H's have exchanged and one in which none of the globally protected H's have exchanged, are typically detected by mass spectrometry during the time course of exchange (*31*−*33*). All the protein mass spectra we collected to generate the SUPREX curves in this work were consistent with EX2 exchange (i.e., only one population of deuterated protein molecules was detected). We note that intermediate H/D exchange behavior between the EX1 and EX2 limits (i.e., when $k_f = \langle k_{int}\rangle$) can be difficult to resolve by mass spectrometry. However, it has been shown that such H/D exchange behavior only leads to small errors in ΔG_f value calculations (*34*).

The urea-induced equilibrium unfolding data that we obtained for S-Pro is shown in Figure 5. The pre- and post-transition baselines used in the normalization of the raw data are denoted by the dotted lines in Figure 5A. The normalized data are shown in Figure 5B. The inset in Figure 5B shows

Table 2: Thermodynamic Parameters for the Proteins and the Protein−Peptide Complexes in this Study

complex	m^a (kcal mol^{-1} M^{-1})	ΔG_f^a (kcal mol^{-1})	r^b	SUPREX K_d^c	literature K_d
abl SH3	0.57 ± 0.12	−5.81 ± 0.16	0.867		
+ 1	0.67 ± 0.10	−6.53 ± 0.20	0.977	57 ± 25 μM	118 μM[d]
+ 2	0.70 ± 0.04	−6.98 ± 0.07	0.997	28 ± 8 μM	28.8 μM[d]
+ 3	0.74 ± 0.06	−7.04 ± 0.12	0.993	25 ± 8 μM	24.1 μM[d]
+ 4	0.87 ± 0.12	−7.88 ± 0.30	0.983	5.2 ± 2.4 μM	5.6 μM[d]
S-Protein	1.06 ± 0.06	−5.17 ± 0.10	0.989		
+ 5	0.70 ± 0.03	−4.67 ± 0.06	0.996	> ∼ 1 mM[e]	∼20 mM[f]
+ 6	0.94 ± 0.10	−5.54 ± 0.14	0.983	250 ± 110 μM	16 μM[g]
+ 7	1.18 ± 0.08	−6.26 ± 0.14	0.993	9.7 ± 3.0 μM	∼7 μM[f]
+ 8	1.15 ± 0.01	−8.07 ± 0.04	0.999	400 ± 70 nM	41 nM[h]
+ 9	1.28 ± 0.07	−9.39 ± 0.22	0.996	34 ± 12 nM	6.3 nM[i]

[a] The m and ΔG_f values were taken from the slopes and y-intercepts (respectively) of the $-RT\ \ln(\langle k_{int}\rangle t/0.693 - 1)$ versus $C^{1/2}_{SUPREX}$ plots generated above. Errors are the standard errors of fitting generated by SigmaPlot. [b] The correlation coefficient obtained from the linear least-squares analysis of each $-RT\ln(\langle k_{int}\rangle t/0.693 - 1)$ versus $C^{1/2}_{SUPREX}$ plot. [c] Values are reported with standard error (i.e., the errors associated with the ΔG_f values in column 3 were propagated through eq 3). [d] Professor Wuyuan Lu, personal communication (University of Maryland). [e] Estimated upper limit of K_d based on our conditions; K_d could not be calculated outright for the reasons stated in the text. [f] K_d estimated from the data in refs *17*, *20*, and *21*. [g] From ref *17*. [h] From ref *18*. [i] The K_d of the S15 peptide of ref *17* extrapolated to 10 °C using their ITC data at higher temperatures with their eq 6. We should note that the S15 peptide from ref *17* is a C-terminally truncated version of our peptide 9; it has been shown that this 5-amino acid truncation does not have a major effect on K_d (*37*).

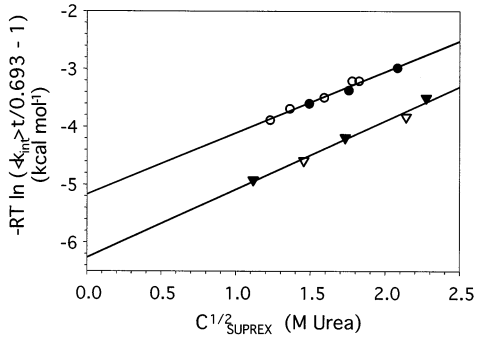

FIGURE 4: The $-RT\ \ln(\langle k_{int}\rangle t/0.693 - 1)$ versus $C^{1/2}_{SUPREX}$ plot for S-Pro in the absence (circles) and in the presence (triangles) of peptide 7. Filled symbols indicate the data points from the SUPREX curves shown in Figure 2. The open symbols indicate the data points from additional SUPREX curves (data not shown). The solid lines are the results of linear least-squares fitting of the data to eq 2.

the plot of ΔG_{app} vs [urea] that was used to calculate the m-value and ΔG_f of S-Pro's unfolding reaction. The slope of this plot, 1.27 ± 0.05 kcal mol^{-1} M^{-1}, was equivalent to the m-value, and the y-intercept, −2.08 ± 0.10 kcal mol^{-1}, was equivalent to ΔG_f.

DISCUSSION

m-Values. An important part of this work was the development of a new method to experimentally determine m-values in SUPREX analyses. In this new method, a series of different SUPREX curves are collected for a given protein sample. Different H/D exchange times (i.e., t values in eq 2) are used to create each SUPREX curve in the series, and a plot of $-RT\ \ln(\langle k_{int}\rangle t/0.693-1)$ versus $C^{1/2}_{SUPREX}$ is generated. Equation 2 predicts that such a plot will be linear and that the slope of the resulting line will correspond to the m-value of the protein under study. The $-RT\ \ln(\langle k_{int}\rangle t/0.693-1)$ versus $C^{1/2}_{SUPREX}$ plots that we generated for the two proteins and nine protein/peptide complexes in this work were in fact linear, and it was possible to extract precise m-values from the data (see Table 2). We note that the relative standard error associated with each m-value determination in Table 2 was generally less than 10%. This precision is typical of that in conventional methods to determine m-values.

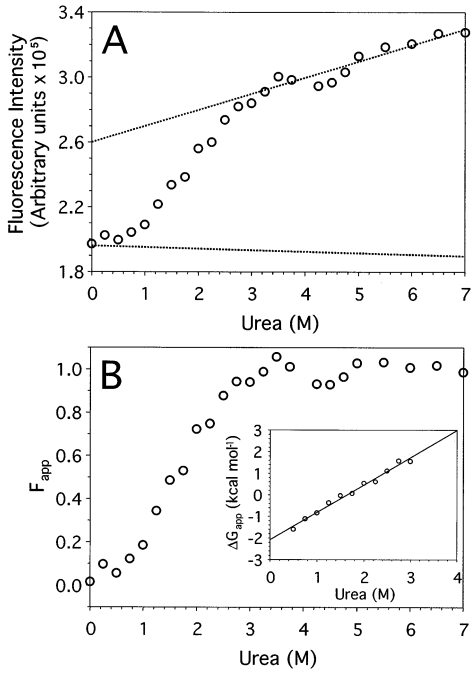

FIGURE 5: (A) Urea-induced equilibrium unfolding curve for S-Pro monitored by fluorescence. The dotted lines represent the urea dependence of the fluorescence intensity of the folded and unfolded forms of S-Pro. (B) The normalized urea-induced equilibrium unfolding curve for S-Pro monitored by fluorescence. The inset shows the ΔG_{app} versus [urea] data for the points in the transition region; the solid line is the result of a linear least-squares fit of the data.

The m-values obtained from our plots of $-RT\ \ln(\langle k_{int}\rangle t/0.693-1)$ versus $C^{1/2}_{SUPREX}$ are expected to be equivalent to those obtained by conventional methods as eq 2 relies on the relationship in eq 7 (see Appendix). Indeed, the SUPREX-derived m-value we obtained for the abl-SH3 domain, 0.57 ± 0.12 kcal mol^{-1} M^{-1}, is in good agreement with a previously reported value of 0.55 kcal mol^{-1} M^{-1} that was calculated using conventional fluorescence denaturation data (*35*). The SUPREX-derived m-value we obtained for S-Pro, 1.06 ± 0.06 kcal mol^{-1} M^{-1}, is also in reasonably good

agreement with the *m*-value of 1.27 ± 0.05 kcal mol^{-1} M^{-1} calculated using the conventional fluorescence denaturation data in this work (see Figure 5). We note that the *m*-values associated with the protein/peptide complexes in this work have not been calculated by conventional techniques. However, the SUPREX-derived *m*-values for these complexes appear to be reasonably accurate since their use in the calculation of the SUPREX-derived K_d values in this work lead to reasonably accurate numbers (see below).

In most cases, the *m*-value for each protein complexed with a peptide was larger than the *m*-value measured for the protein alone. The large *m*-values of each protein−peptide complex can in part be attributed to the reduction of solvent accessible surface area in each protein upon peptide binding. It has been shown that the amount of solvent accessible surface area buried upon protein folding is directly proportional to the *m*-value of a protein folding reaction and that the *m*-value of a protein folding reaction can be estimated by the number of amino acids in a protein (i.e., 0.013 kcal mol^{-1} M^{-1} per amino acid residue) (*26*). According to such an estimate, the *m*-values of the protein-peptide complexes in this work should be increased by ∼0.1−0.2 kcal mol^{-1} M^{-1} over what they would be for the protein alone. The changes we observed were generally in this range. Our results in Table 2 also indicate that for each protein−peptide system there was a reasonably good correlation between the magnitude of the measured *m*-value and the strength of the protein−peptide binding interaction. The largest *m*-values were obtained when the abl-SH3 domain and S-Pro were complexed with the tightest binding peptide ligands. This apparent increase in cooperativity of the S-Pro and abl-SH3 domain folding reactions in the presence of tight binding peptides may be due to the more efficient packing of the amino acid side chains at the protein−peptide interfaces in these complexes.

The *m*-value we determined for the S-Pro/peptide 5 complex was unexpectedly low. No binding was detected in our experiments on this complex (see below). However, we expected the *m*-value for this complex to be equivalent to the *m*-value determined for the S-Pro alone. It appears that the presence of peptide 5 decreased the cooperativity of S-Pro's folding reaction. The reason for this is unknown; however, this behavior appears to be unique to the S-Pro/peptide 5 complex.

K_d Values. The SUPREX technique accurately ranked the relative binding affinities of all the different peptides in both of the protein systems studied here, and the SUPREX-derived K_d values we obtained for six of the nine complexes in this study were in excellent agreement (i.e., within 5-fold) of previously reported values. For two of the nine protein−peptide complexes in this study the SUPREX-derived K_d values obtained were within ∼10-fold of the reported values, and for one complex, the S-Pro/peptide 5 complex, only a lower limit for the K_d value could be established. The uncertainties presented with the SUPREX K_d values in Table 2 were obtained by the propagation of the linear least-squares fitting error from ΔG_f (column 3, Table 2) through eq 3. These errors ranged from 17 to 46% and were generally on the order of 30%. The magnitude of this error is close to that of conventional techniques. For example, the errors associated with the literature K_d values in Table 2 are in the range of ∼5−25% (*18*, *21*).

The average deviation of replicate measurements is typically a good esitmate of the precision of a technique. Replicate K_d values can be calculated from the multiple SUPREX curves that we collected for each protein and protein−peptide complex. If the *m*-values from Table 2 are used in eq 2 to calculate ΔG_f values from the individual SUPREX curves we recorded at different exchange times for each protein−peptide complex, then at least four independent calculations of ΔG_f values can be made for each protein−peptide complex. The resulting ΔG_f values can be used to calculate at least four independent $\Delta\Delta G_f$ values, and the resulting $\Delta\Delta G_f$ values can ultimately be used to calculate at least four independent K_d values for each protein−peptide complex. Treatment of our data in this fashion results in average K_d values that are essentially the same as those reported in Table 2. The average deviations of our K_d values calculated in this fashion ranged from 2.5 to 24%, and they were typically on the order of ∼10%.

In theory, the SUPREX technique described here for measuring the K_d values of protein−peptide complexes should be amenable to an unbounded range of K_d values. The technique relies on detecting the increase in a protein's ΔG_f value upon ligand binding (i.e., measuring $\Delta\Delta G_f$). In the case of tightly bound protein−peptide complexes, such as the S-Pro/peptide 9 complex with a reported K_d of 6.3 nM, large $\Delta\Delta G_f$ values are expected upon peptide binding. However, in the case of weakly bound complexes, such as the S-Pro/peptide 5 complex with an estimated K_d of 20 mM, the measured $\Delta\Delta G_f$ values can be small and difficult to measure. According to eq 3, it is possible to increase the $\Delta\Delta G_f$ value for a given protein−peptide complex by increasing the amount of free ligand in the assay. However, the high peptide concentrations required to produce a measurable $\Delta\Delta G_f$ value (i.e., $\Delta\Delta G_f > \sim 0.5$ kcal mol^{-1}) can still be difficult to achieve experimentally. For example, in the case of the S-Pro/peptide 5 complex with a K_d of 20 mM, a 30 mM peptide concentration is required to produce a $\Delta\Delta G_f$ value on the order of 0.5 kcal mol^{-1}. Such a high peptide concentration was not accessible in our experiments.

The SUPREX-derived K_d values for the S-Pro/peptide 6 and the S-Pro/peptide 8 complexes were only within about an order of magnitude of previously reported K_d values. If the reported K_d values for the S-Pro complexes of peptide 6 and peptide 8 are accurate then the K_d values we determined for these complexes by SUPREX are arguably high. The amino acid sequences of peptides 6 and 8 are very closely related to amino acid sequence of peptide 9, and it is interesting to note that the SUPREX-derived K_d values we measured for these three pepitde ligands were all between 5- and 20-fold high. An important assumption in this work is that the peptide ligands do not bind the denatured state of the protein. Significant denatured state binding and/or nonlinear effects at low [Denaturant] in our $-RT\ \ln(\langle k_{int}\rangle t/0.693 - 1)$ versus $C_{SUPREX}^{1/2}$ plots (see Figures 3 and 4) could potentially account for the large K_d values determined in our SUPREX experiments on the S-Pro and peptides 6, 8, and 9. Such nonlinear effects at low [urea] have been noted in previous peptide binding studies with S-Pro (*19*).

The accuracy of the SUPREX-derived K_d values in this work was not dependent on the accuracy of the SUPREX-derived ΔG_f values in this work. The SUPREX-derived ΔG_f

values we obtained for the abl-SH3 domain and S-Pro were -5.81 ± 0.16 and -5.17 ± 0.10 kcal mol^{-1} (respectively). These ΔG_f values are approximately 2−3 kcal mol^{-1} larger than ΔG_f values for these proteins obtained using conventional techniques. The discrepancy may be due to the $\langle k_{int} \rangle$ values used in our SUPREX analyses. In our calculation of ΔG_f values using eq 2, the intrinsic exchange rates of all the globally protected amide protons in each protein and protein−peptide complex were estimated by $\langle k_{int} \rangle$ using SPHERE, a program based on the model peptide data of Bai et al. (*28*). Our estimated $\langle k_{int} \rangle$ values may be wrong for two reasons. One reason is related to the fact that all the k_{int} values of all the amide protons in each protein are factored into our $\langle k_{int} \rangle$ value estimates. Clearly, only a subset of these amide protons are "globally" protected. The most accurate $\langle k_{int} \rangle$ values would be obtained if only the k_{int} values of these globally protected amide protons in each protein were factored into our $\langle k_{int} \rangle$ value estimates. Unfortunatley, in our SUPREX experiment it is not possible to determine which amide protons are globally protected and which are not. A second reason that our estimated $\langle k_{int} \rangle$ values may be wrong is that the k_{int} values calculated from the SPHERE program are based on amide exchange occurring in a completely random coil-like structure. The chemically denatured states of the proteins in this work may not be well modeled by a random coil-like structure.

Clearly, the accuracy of our SUPREX-derived ΔG_f values is dependent on the $\langle k_{int} \rangle$ value used in our calculations. However, it is important to note that the $\Delta\Delta G_f$ values used to generate K_d values of the protein−peptide complexes in this work are not sensitive to errors in $\langle k_{int} \rangle$. This is because the $\langle k_{int} \rangle$ values for the proteins in this study are not expected to change upon ligand binding. Therefore, the $\langle k_{int} \rangle$ term in eq 2 is canceled out when the equation is used to calculate $\Delta\Delta G_f$ values. This is confirmed by the good agreement between our SUPREX-derived K_d values in Table 2 and those reported in the literature.

APPENDIX

The SUPREX technique relies on the hydrogen/deuterium (H/D) exchange reaction of globally protected amide protons in proteins. For proteins with equilibrium unfolding behavior that is well-modeled by a two state process (i.e., no partially folded intermediate states are populated) the H/D exchange reaction can be described by eq 8 (*10*, *34*, *38*, *39*):

$$P_{cl}^{H} \underset{k_{cl}}{\overset{k_{op}}{\rightleftharpoons}} P_{op}^{H} \xrightarrow{k_{int}} P_{op}^{D} \tag{8}$$

In eq 8 P_{cl}^{H} is a closed, H/D exchange incompetent form of the protein, P_{op}^{H} is an open, H/D exchange competent form of the protein before H/D exchange has occurred, P_{op}^{D} is an open, H/D exchange competent form of the protein after H/D exchange has occurred, k_{op} and k_{cl} are the rate constants for the opening and closing reactions of the protein (respectively), and k_{int} is the intrinsic, chemical exchange rate for an amide proton. Note that there is no reverse arrow in eq 8 since the reaction is performed in D_2O. The observed H/D exchange rate constant, k_{ex}, can be written in the form of eq 9.

$$k_{ex} = \frac{k_{op} k_{int}}{k_{op} + k_{cl} + k_{int}} \tag{9}$$

For folded proteins at the EX2 limit of H/D exchange, $k_{cl} \gg k_{op}$ and $k_{cl} \gg k_{int}$, and eq 9 reduces to eq 10. If K_{op} is defined

$$k_{ex} = \frac{k_{op} k_{int}}{k_{cl}} \tag{10}$$

as the equilibrium constant for the opening reaction, then k_{op}/k_{cl} in eq 10 can be rewritten in the form of eq 11. In the

$$k_{ex} = K_{op} k_{int} \tag{11}$$

case of a folded protein $K_{op} \ll 1$, and eq 11 can be rewritten in the following form:

$$k_{ex} = \frac{K_{op} k_{int}}{K_{op} + 1} \tag{12}$$

For amide protons that exchange through a global unfolding mechanism, $1/K_{op}$ or K_{cl} (i.e., the equilibrium constant for the closing reaction) is equal to K_f, the equilibrium constant for the global folding reaction of the protein in question. Substitution of $K_{op} = 1/K_f$ into eq 12 yields eq 13. Solving

$$k_{ex} = \frac{k_{int}}{K_f + 1} \tag{13}$$

eq 13 for K_f yields eq 14, which is an expression for the equilibrium constant for a protein's folding reaction in terms of k_{int} and k_{ex}:

$$K_f = \frac{k_{int}}{k_{ex}} - 1 \tag{14}$$

At the transition midpoint of a SUPREX curve (i.e., at $C_{SUPREX}^{1/2}$), the H/D exchange reaction has progressed to one half-life. Therefore, eq 15 can be used to describe the relationship between the H/D exchange time, t, and k_{ex}.

$$k_{ex} = 0.693/t \tag{15}$$

Substitution of eq 15 into eq 14 yields eq 16 if the k_{int} values for all globally exchanging hydrogens are approximated by $\langle k_{int} \rangle$.

$$K_f = \frac{\langle k_{int} \rangle t}{0.693} - 1 \tag{16}$$

One of the most common methods for the analysis of traditional solvent-induced, equilibrium denaturation curves is the linear extrapolation method (LEM) (*22*). The LEM is based on eq 17.

$$-RT \ln K_f = m[\text{Denaturant}] + \Delta G_f \tag{17}$$

In eq 17, R is the gas constant, T is the temperature in Kelvin, K_f is the apparent equilibrium folding constant, m is $\delta\Delta G_f/\delta$[Denaturant], [Denaturant] is the molar denaturant concentration, and ΔG_f is the folding free energy of the protein in the absence of denaturant. Equation 17 is generally valid for proteins that exhibit two-state equilibrium unfolding behavior.

Equations 16 and 17 can be combined to yield eq 18 if [Denaturant] is replaced with $C^{1/2}_{SUPREX}$, which is simply the [Denaturant] at the midpoint of the SUPREX transition (note that $C^{1/2}_{SUPREX}$ is not equal to the midpoint of a traditional denaturation curve; see refs *10* and *13*). Equation 18

$$-RT \ln\left(\frac{\langle k_{int}\rangle t}{0.693} - 1\right) = mC^{1/2}_{SUPREX} + \Delta G_f \qquad (18)$$

describes the SUPREX behavior of monomeric proteins such as the ones in this study. Note that eq 2, presented in Materials and Methods, is a more general form of eq 18 as it includes terms for multimeric state and protein concentration (*40*, *41*). Equation 2 is generally applicable to the SUPREX analysis of both monomeric and multimeric proteins provided that the two main assumptions inherent in the above derivation hold true (i.e., that the protein under study is under EX2 exchange conditions and that the protein is a two-state folder).

REFERENCES

1. Bouley, R., Pérodin, J., Plante, H., Rihakova, L., Bernier, S. G., Maletínská, L., Guillemette, G., and Escher, E. (1998) *Eur. J. Pharm. 343*, 323−331.
2. Zhang, Y. L., Marepalli, H. R., Lu, H.-f., Becker, J. M., and Naider, F. (1998) *Biochemistry 37*, 12465−12476.
3. Kazantzis, A., Waldner, M., Taylor, J. W., and Kapurniotu, A. (2002) *Eur. J. Biochem. 269*, 780−791.
4. Loor, F., Tiberghien, F., Wenandy, T., Didier, A., and Traber, R. (2002) *J. Med. Chem. 45*, 4598−4612.
5. Wesley, V. J., Hawtin, S. R., Howard, H. C., and Wheatley, M. (2002) *Biochemistry 41*, 5086−5092.
6. Pisabarro, M. T., and Serrano, L. (1996) *Biochemistry 35*, 10634−10640.
7. Sparks, A. B., Rider, J. E., Hoffman, N. G., Fowlkes, D. M., Quilliam, L. A., and Kay, B. K. (1996) *Proc. Natl. Acad. Sci. U.S.A.* 93, 1540−1544.
8. Dalharno, D. C., Botfield, M. C., and Rickles, R. J. (1997) *Biopolymers 43*, 383−400.
9. Donaldson, L. W., Gish, G., Pawson, T., Kay, L. E., and Forman-Kay, J. D. (2002*) Proc. Natl. Acad. Sci. U.S.A. 99*, 14053−14058.
10. Ghaemmaghami, S., Fitzgerald, M. C., and Oas, T. G. (2000) *Proc. Natl. Acad. Sci. U.S.A. 97*, 8296−8301.
11. Ghaemmaghami, S., and Oas, T. G. (2001) *Nat. Struct. Biol. 8*, 879−882.
12. Powell, K. D., and Fitzgerald, M. C. (2001) *Anal. Chem. 73*, 3300−3304.
13. Powell, K. D., Wales, T. E., and Fitzgerald, M. C. (2002) *Protein Sci. 11*, 841−851.
14. Powell, K. D., Wang, M. Z., Silinski, P., Ma, L., Wales, T. E., Dai, S. Y., Warner, A. H., Yang, X., and Fitzgerald, M. C. (2003) *Anal. Chim. Acta*, in press.
15. Powell, K. D., Ghaemmaghami, S., Wang, M. Z., Ma, L., Oas, T. G., and Fitzgerald, M. C. (2002) *J. Am. Chem. Soc. 124*, 10256−10257.
16. Connelly, P. R., Varadarajan, R., Sturtevant, J. M., and Richards, F. M. (1990) *Biochemistry 29*, 6108−6114.
17. Varadarajan, R., Connelly, P. R., Sturtevant, J. M., and Richards, F. M. (1992) *Biochemistry 31*, 1421−1426.
18. Thomson, J., Ratnaparkhi, G. S., Varadarajan, R., Sturtevant, J. M., and Richards, F. M. (1994) *Biochemistry 33*, 8587−8593.
19. Goldberg, J. M., and Baldwin, R. L. (1998) *Biochemistry 37*, 2546−2555.
20. Goldberg, J. M., and Baldwin, R. L. (1998) *Biochemistry 37*, 2556−2563.
21. Goldberg, J. M., and Baldwin, R. L. (1999) *Proc. Natl. Acad. Sci. U.S.A. 96*, 2019−2024.
22. Pace, C. N. (1986) *Methods Enzymol. 131*, 266−280.
23. Glasoe, P. K., and Long, F. A. (1960) *J. Phys. Chem. 64*, 188−190.
24. Richards, F. M., and Vithayathil, P. J. (1959) *J. Biol. Chem. 234*, 1459−1465.
25. Schnölzer, M., Alewood, P., Jones, A., Alewood, D., and Kent, S. B. H. (1992*) Int. J. Pept. Protein Res. 40*, 180−193.
26. Myers, J. K., Pace, C. N., and Scholtz, J. M. (1995) *Protein Sci. 4*, 2138−2148.
27. Zhang, Y.-Z. (1995) Ph.D. Thesis, Structural Biology and Molecular Biophysics, University of Pennsylvania, PA.
28. Bai, Y., Milne, J. S., Mayne, L., and Englander, S. W. (1993) *Proteins 17*, 75−86.
29. Schellman, J. A. (1975) *Biopolymers 14*, 999−1018.
30. Segel, I. H. *Enzyme Kinetics*; John Wiley & Sons: New York, 1975.
31. Miranker, A., Robinson, C. V., Radford, S. E., Aplin, R. T., and Dobson, C. M. (1993) *Science 262*, 896−900.
32. Smith, D. L., Deng, Y., and Zhang, Z. (1997) *J. Mass Spectrom. 32*, 135−146.
33. Arrington, C. B., Teesch, L. M., and Robertson, A. D. (1999) *J. Mol. Biol. 285*, 1265−1275.
34. Bai, Y., Milne, J. S., Mayne, L., and Englander, S. W. (1994) *Proteins 20*, 4−14.
35. Filimonov, V. V., Azuaga, A. I., Viguera, A. R., Serrano, L., and Mateo, P. L. (1999) *Biophys. Chem. 77*, 195−208.
36. Neira, J. L., Sevilla, P., Menéndez, M., Bruix, M., and Rico, M. (1999) *J. Mol. Biol. 285*, 627−643.
37. Mitchinson, C. and Baldwin, R. L. (1986) *Proteins 1*, 23−33.
38. Hvidt, A., and Nielsen, S. O. (1966) *Adv. Prot. Chem. 21*, 287−386.
39. Roder, H., Wagner, G., and Wüthrich, K. (1985) *Biochemistry 24*, 7396−7407.
40. Breslauer, K. J. (1995) *Methods Enzymol. 259*, 221−242.
41. Backmann, J., Schäfer, G., Wyns, L., and Bönisch, H. (1998) *J. Mol. Biol. 248*, 817−833.

BI034096W